SIMULATION STUDIES OF A GPC CONTROLLER FOR A HYDROELECTRIC PLANT

G A Muñoz-Hernández

Instituto Tecnológico de Puebla

D I Jones

formerly with

School of Electronic Engineering

University of Wales, Bangor

Corresponding author:

Dr D I Jones
GWEFR Cyf
Pant Hywel
Penisarwaun
Caernarfon
Gwynedd LL55 3PG
United Kingdom

tel: +44 (0)1286 400250

e-mail: dewi@gwefr.co.uk

web: www.gwefr.co.uk

Abstract.

In this paper, the performance of constrained Generalized Predictive Control (CGPC) is investigated on a comprehensive nonlinear multivariable simulation of the Dinorwig pumped - storage hydroelectric power station. The responses of the system are compared with those of the classic PI controller, as currently implemented on the plant. The results show that CGPC offers significantly better performance over the whole operating envelope. Fixed-parameter CGPC produces a faster primary response and better steady-state accuracy when the station is operating with a single unit, while also preserving stability when the operating conditions change as multiple units come on-line. It can accommodate large amplitude ramp power changes in combination with feed-forward control. It is less sensitive than PI to changes in hydraulic head and gives better power-tracking when units operate in frequency-control mode. Finally, the computational time of the CGPC algorithm is investigated.

Keywords.

Hydroelectric power; power station control; pumped storage plant; simulation; model predictive control.

1 Introduction

Dinorwig is a large pumped-storage hydroelectric scheme located in North Wales, which is owned by the First Hydro Company. The station has six 300MW rated turbines, driving synchronous generators to provide peak-lopping and ancillary services to the national grid. In a recent paper Muñoz Hernández and Jones (2006) describe how the plant's dynamic performance could be improved, over the whole operating envelope, by using Generalised Predictive Control (GPC) instead of the PI control currently implemented. In a fast-response hydroelectric station, the dynamic operating point is largely determined by the flow in the main tunnel and hence the number of units on-line at a given time. It is generally the case that such plant use a fixed parameter PI governor that is tuned to avoid instability at the worst-case operating point, which occurs when all units are generating. However, the operational rationale for a pumped-storage station necessarily means that it spends a substantial portion of its life generating on only one or two units. In these circumstances, the conservatively tuned governors do not give optimal power delivery. The motivation for developing the GPC controller was to obtain better performance over the whole operational range, rather than accept the compromise imposed by separate PI controllers on individual units. In (Muñoz Hernández and Jones, 2006), it was shown that constrained GPC (CGPC), which incorporates saturation and rate limits on the control variables, has the potential to achieve this goal. The purpose of this paper is to remove the modelling restrictions in that work in order to confirm the superiority of CGPC under conditions not previously considered. So the controller used here is the one described in (Muñoz Hernández and Jones, 2006) but applied now to a full nonlinear simulation of the plant, instead of the MIMO small-signal linearised model used to perform the design. The accuracy of the full model, as derived by Mansoor *et al* (2000), has been verified with respect to measured plant responses. As well as its small-step response, the CGPC controller is assessed in several other situations:

- When large amplitude ramp inputs are applied;
- When there are different numbers of units on line;
- When the hydraulic head changes with the water level in the upper reservoir;
- When the stiffness and damping of the Grid change during frequency-control mode.

The impact on real-time performance of the quadratic programming (QP) computation needed to implement CGPC is also discussed. In the next two sections, the nonlinear plant model is described and the theory of multivariable CGPC is summarised. Next, the results of the simulation studies are presented. Finally, conclusions are drawn with respect to the performance of CGPC.

2 The Dinorwig plant.

Figure 1 is a schematic diagram of the power station (showing only 2 of the 6 turbines). There is a single tunnel that draws water from an upper reservoir into a manifold where the flow is split into six penstocks. Each penstock is equipped with a turbine/generator unit which produces power under the control of a set of guide vanes that regulate the flow. At present, individual PI feedback loops, implemented on PLC governors, are used to control the guide vanes and hence the electrical power output. Generally, the units work in one of two modes – either regulating power to a set-point or in frequency control mode, where the reference input to the power loop depends on the grid frequency deviation from its nominal value of 50Hz.

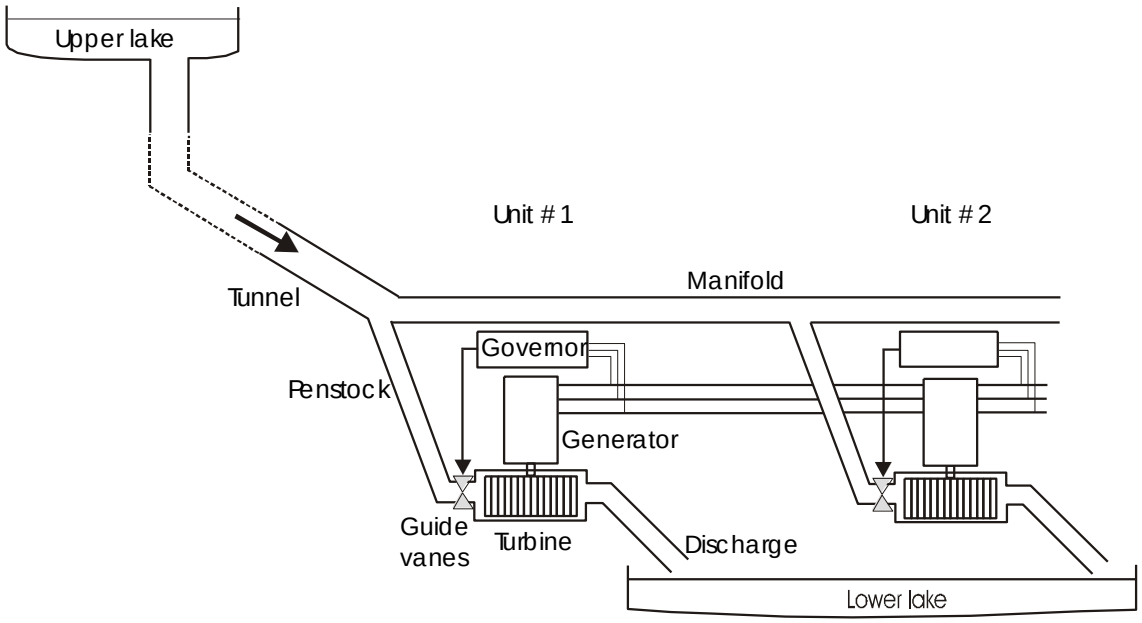

Figure 1 Schematic of the pumped storage plant (shown for 2 units only).

The core of the plant model is the hydraulic subsystem whose block diagram is shown in Figure 2, where q represents flow, P_m represents mechanical power and h represents head (pressure). This is a per-unit model, based on the derivation in (IEEE Working group, 1992) with the power and frequency variables normalised to 300MW and 50Hz, respectively. The steady-state relationship between the flow through a turbine, the pressure at the inlet and its mechanical power output is given by:

$$P_m = A_t h q \tag{1}$$

where A_t is the turbine constant. The flow is a function of the guide vane opening (G):

$$q = G\sqrt{h} \tag{2}$$

The nonlinear relationships (1) and (2) cause the effective gain of the plant (i.e. change in generated power with guide vane opening) to vary significantly with flow and head. They also show that reducing steady state power output requires the guide vanes to be closed. Doing so causes a transient increase in the turbine inlet pressure whose amplitude depends on the rate of closure. However, as a consequence of the inertia of the moving water column, there is no change in the instantaneous flow and there is consequently a transient increase in the power

output, which is the opposite of the desired effect. This well-known non-minimum phase (NMP) characteristic imposes fundamental limits on the dynamic performance of fast-response hydroelectric plant.

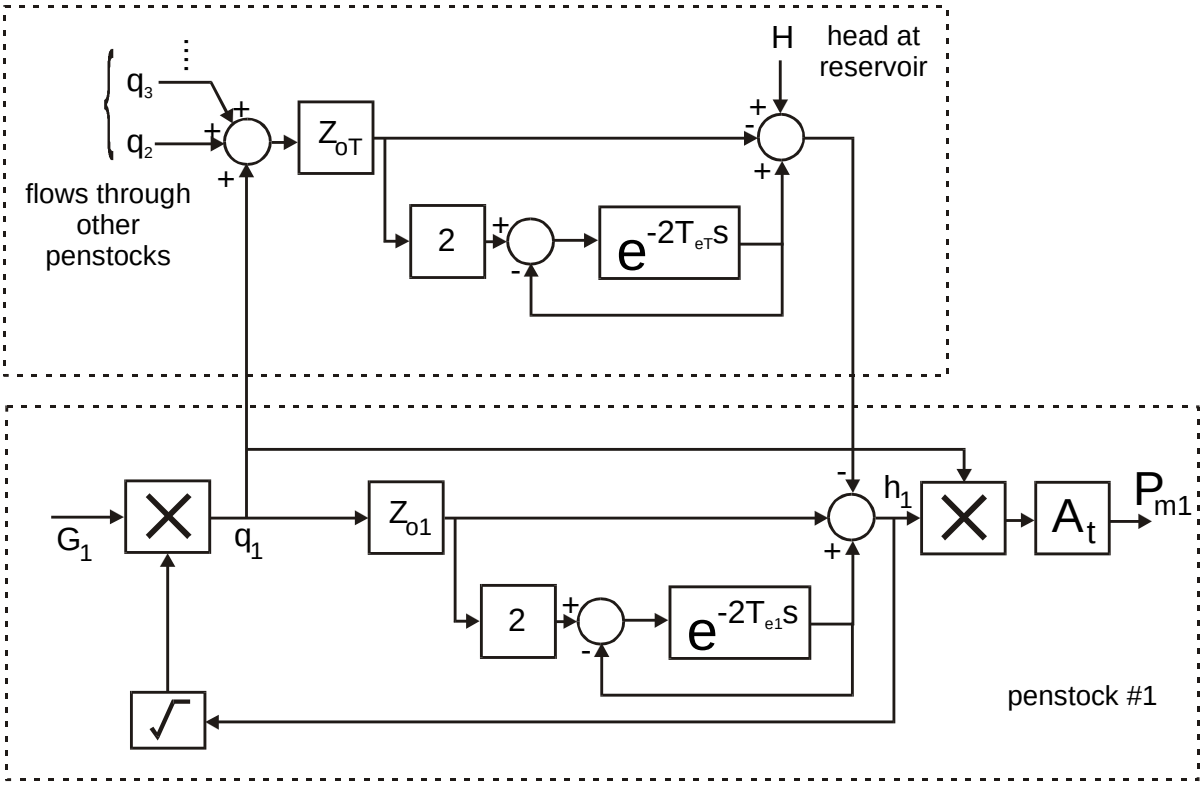

Figure 2 The core hydraulic model for the plant (only 1 penstock shown).

The hydraulic coupling, i.e. a change of flow through one turbine reacting upon the others, is represented by the summing junction in Figure 2, which adds the individual penstock flows. Coupling has a fundamental effect on the dynamics (Jones, 1999) and was represented in the linearised plant model (Muñoz Hernández and Jones, 2006) by using different transfer functions according to the number of units on-line. The surge impedance and time delay blocks in Figure 2 represent the effect of travelling waves in the penstocks and tunnel due to elasticity of the conduit walls and compressibility of water. This can produce poorly-damped oscillations in the power output in response to sharp changes in guide vane angle. The variables Z_{oT} and Z_{o1} are the characteristic impedances of the tunnel and penstock #1, respectively. T_{eT} and T_{e1} are the corresponding travelling wave times. Another feature of

Figure 2 is the head (H) of the upper reservoir. This obviously affects the steady-state performance of the plant but it also acts as a gain term on the transient response, which is faster when the reservoir is full. The reservoir head usually varies with the time of day. The simulation also includes the surge tank dynamics, a no-load flow to represent turbine fixed power loss, the effect of nonlinear head loss due to friction in the conduit and a speed deviation damping term; these are omitted from Figure 2 for clarity. Altogether, this is a more complete and accurate model of the hydraulic subsystem than used in (Muñoz Hernández and Jones, 2006) where the linearised multivariable model excluded the elastic water column effects and all nonlinearities. The hydraulic subsystem is connected to the other subsystems to form the complete plant model shown in Figure 3 where ω is the generator speed, P_e is the electrical power and P_{ed} its demanded value. The additional subsystems are described in (Mansoor, Jones et al., 2000) and comprise:

- the usual 'swing' equations (Kundur, 1994) to represent the turbine/generator as a second order transfer function; this introduces fast, poorly-damped transients due to electrical synchronisation;
- the dynamics of the guide vanes and their two-stage (oil) hydraulic actuator, modelled as two cascaded first-order transfer functions;
- a first-order filter on the measurement of electrical power.

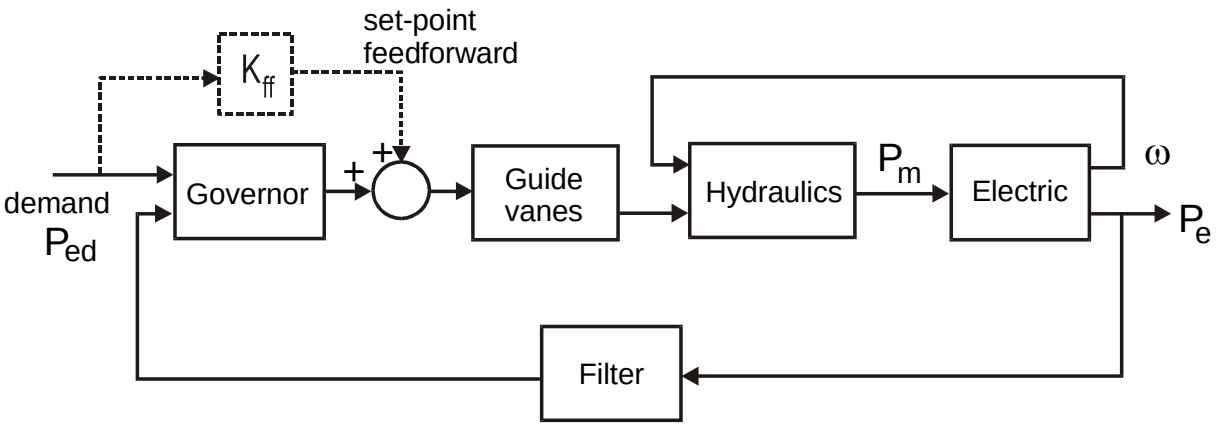

Figure 3 The subsystems of the hydroelectric plant.

Finally, the model used here includes a transfer function for the national grid (Anderson and Mirheydar, 1990), (Jones, 2004) whereas the analysis in (Muñoz Hernández and Jones, 2006) assumed a power system with an infinite bus.

3 MIMO Generalised Predictive Control

Model Based Predictive Control (MBPC) is the general name of a class of controllers, one popular variant of which is Generalized Predictive Control (GPC) as considered here. The GPC method, first proposed by Clarke *et al* (1987), (1987) has been successfully implemented in many industrial applications (Richalet, 1993), (Camacho and Bordons, 1999), (Maciejowski, 2001) but the recent work by Muñoz-Hernández and Jones (2004; 2004; 2006) is believed to be its first application to hydroelectric plant. As the name MBPC suggests, the main characteristic of the method is a computation of the future output ($\hat{y}$) of the plant from its present state using an internal 'predictive' model - usually a rather simple one. This is done for a specified number (N_u) of samples of the control (u) into the future, known as the 'control horizon'. The predicted error of the output from some desirable reference trajectory (w) can then be computed. An optimization problem is set up and solved for the future control which minimizes a cost functional of the predicted error and the control exerted (these being conflicting requirements). Only the first of the optimized control values is actually applied to the physical plant because, at the next sample, the whole procedure is performed once more to generate a new control. The quadratic cost function to be minimized at each sample time t is:

$$J(N_1, N_2, N_u) = \sum_{j=N_1}^{N_2} \left[\hat{y}(t+j \mid t) - w(t+j)\right]^2 Q + \sum_{j=1}^{N_u} \left[\Delta u\left(t+j-1\right)\right]^2 R \quad (3)$$

where $\hat{y}(t+j|t)$ is the optimum predicted output of the plant at sample j, Δ is the $(1\text{-}q^{-1})$ operator, N_1 and N_2 are the start and end of the output prediction horizon, $w(t+j)$ is the future

reference trajectory and Q and R are positive definite weighting matrices which trade-off output accuracy and control effort. The CGPC controller (Muñoz Hernández and Jones, 2006) uses $R = \mathbf{I}\lambda$ and $Q = \mathbf{I}$ so that the scalar λ plays the role of an inverse loop gain – a high value of λ penalises the control term in (3) which results in reduced control effort at the expense of increased tracking error. The reference trajectory $w(t+j)$ is fixed to the input demand value.

The discrete-time predictive model is conveniently represented in the CARIMA (Controller Auto-Regressive Moving-Average with Integrator) form with m inputs, n outputs and input delay d:

$$A(q^{-1})y(t) = q^{-d}B(q^{-1})u(t-1) + C(q^{-1})\frac{e(t)}{1-q^{-1}} \qquad (4)$$

where $\mathbf{A}(q^{-1})$ and $\mathbf{C}(q^{-1})$ are matrices of monic polynomials of order n x n and $\mathbf{B}(q^{-1})$ is a polynomial matrix of order n x m; e(t) is the output error. As described in(Muñoz Hernández and Jones, 2006), the matrices A, B and C were derived from a simplified version of the plant model and fixed for the operating condition 0.95p.u., 6 units in operation and a sample time $T = 0.25$s:

$$A_6(q^{-1}) = 1 - 2.5442q^{-1} + 2.4304q^{-2} - 1.0728q^{-3} + 0.2153q^{-4} - 0.0157q^{-5} \qquad (5)$$

$$B_6(q^{-1}) = 0.2904q^{-4} - 0.5234q^{-5} + 0.3175q^{-6} - 0.076q^{-7} + 0.0061q^{-8} \qquad (6)$$

$$b_6(q^{-1}) = -0.0476q^{-1} + 0.0078q^{-2} + 0.0886q^{-3} - 0.0437q^{-4} - 0.0051q^{-5} \qquad (7)$$

where A_6, B_6 are the diagonal elements and b_6 are the off-diagonal elements. It is clear that the accuracy of this predictive model is limited and depends on the operating point but it has the merit of being quick to compute, which is particularly important in the case of constrained MBPC. In fact, it was found (Muñoz Hernández and Jones, 2006) that using more complex predictive models produced only minor improvement in performance and (5) – (7) were used throughout.

It is common to formulate control laws on the assumption that all plant states and controls possess an unlimited range. In this case, GPC provides a computationally efficient solution for the optimum control signal:

$$u^* = \arg\min_{u}(J) \tag{8}$$

In practice, all plants are subject to constraints, typically for constructional and safety reasons. In MBPC, three types of constraint are usually considered – saturation of control signals, rate limits on control signals and limits on output values – as follows:

$$\begin{aligned} &\text{control limit} && \underline{u} \le u(t) \le \overline{u} \\ &\text{control rate limit} && \underline{\Delta u} \le u(t) - u(t-1) \le \overline{\Delta u} \\ &\text{output limit} && \underline{y} \le y(t) \le \overline{y} \end{aligned} \tag{9}$$

Here, the control rate is limited to $-0.2 \le \Delta u \le 0.2$p.u. An effective strategy for the control saturation limit is to cap its value at each sample instant according to:

$$\begin{aligned} &0 \le u \le P_{ed} / A_t && \dot{P}_{ed} > 0 \\ &P_{ed} / A_t \le u \le 1 / A_t && \dot{P}_{ed} < 0 \end{aligned} \tag{10}$$

i.e. the control is never allowed to exceed the value set by the demanded power (P_{ed}). The inclusion of constraints makes (8) a quadratic programming problem. This is solved at each sample instant using an interior-reflective Newton method with the unconstrained solution as an initial guess. This iterative method increases the computation time substantially compared to unconstrained GPC.

4 Small step responses

Here, the small-step CGPC responses for the full plant model are compared with the responses produced by the PI controller currently in use, which is configured with gain settings of

K_p = 0.1 and K_i = 0.12, a control rate limit of ±0.2p.u.and control saturation fixed at 1p.u. with anti-windup safeguard (Muñoz Hernández and Jones, 2006). Figure 4 shows a 0.04p.u. (12MW) step demand in power being applied to a single unit, the remaining units being off-line. All the CGPC responses are faster and have a smaller NMP under-shoot than produced by the PI controller, which is consistent with previous findings. CGPC also produces a smooth response, whereas the PI controller causes rapid pressure variations in the elastic water column leading to the power oscillations seen in Figure 4. In fact, this prevents further increase in the PI loop gain. None of the responses activate either rate or saturation constraints. Figure 4 indicates that λ in the range 150 - 250 gives a well-damped response and a substantial improvement in primary response compared to the PI controller. The reduced value of λ, compared to the original design value of 350, is required in order to counteract the delay introduced by inclusion of the elastic water column in the plant model. A value of N_u = 10 samples was chosen because longer control horizons used significantly more computational effort while producing only small improvements in the response.

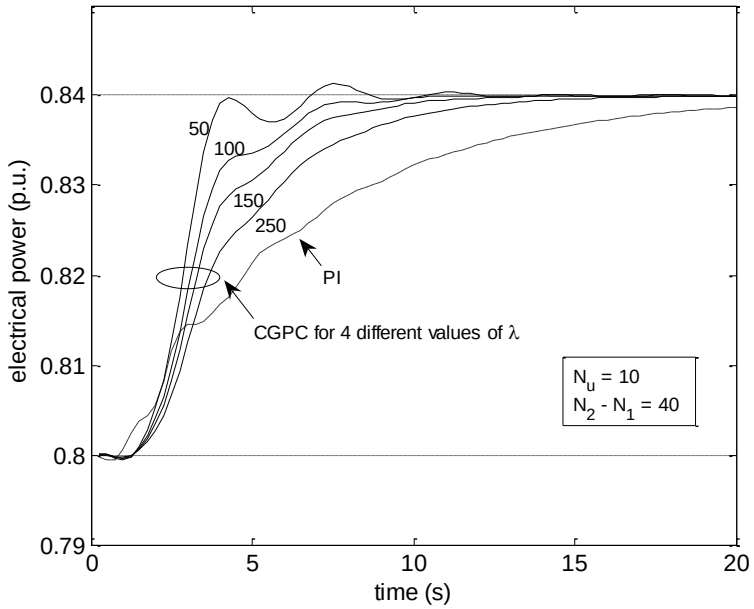

Figure 4 Comparison of CGPC and PI responses when one unit has a small step demand in power and the remaining 5 units are off-line.

Figure 5 shows a 0.04p.u. step demand in power being applied to Unit 1 with the remaining 5 units generating at fixed 0.8p.u. Note the cross-coupling perturbations which affect all 5 other Units identically and the consequent deterioration in stability (Jones, 1999) – a small overshoot is now to be seen in the λ = 150 case.

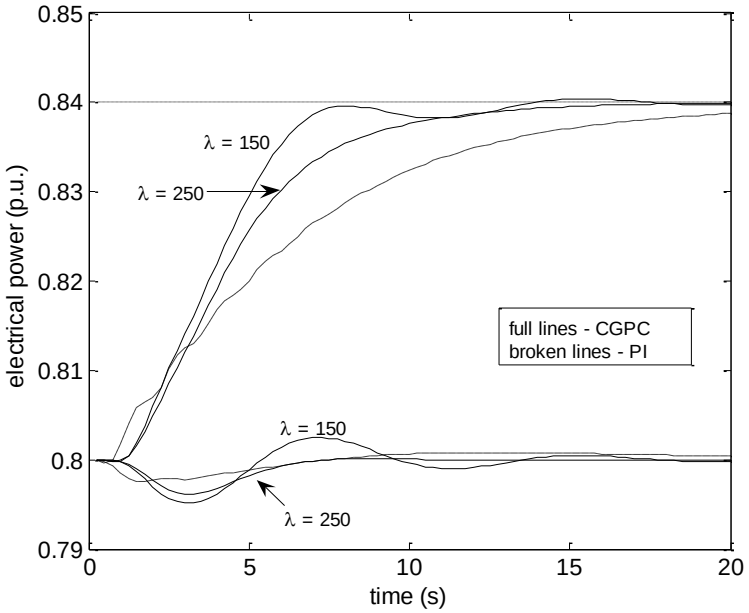

Figure 5 Comparison of CGPC and PI responses when one unit has a small step demand in power while the remaining 5 units are generating at 0.8p.u.

Finally, the small-step response when all 6 units react together to an identical power demand is presented in Figure 6.

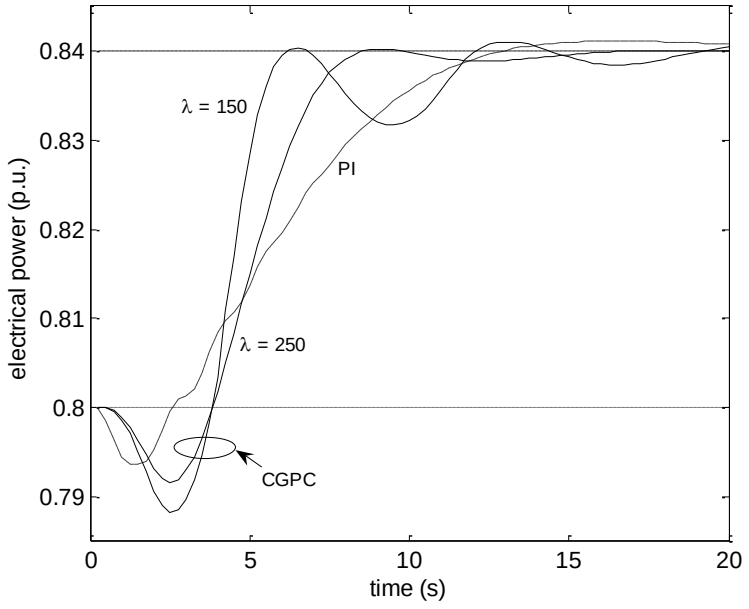

(a)

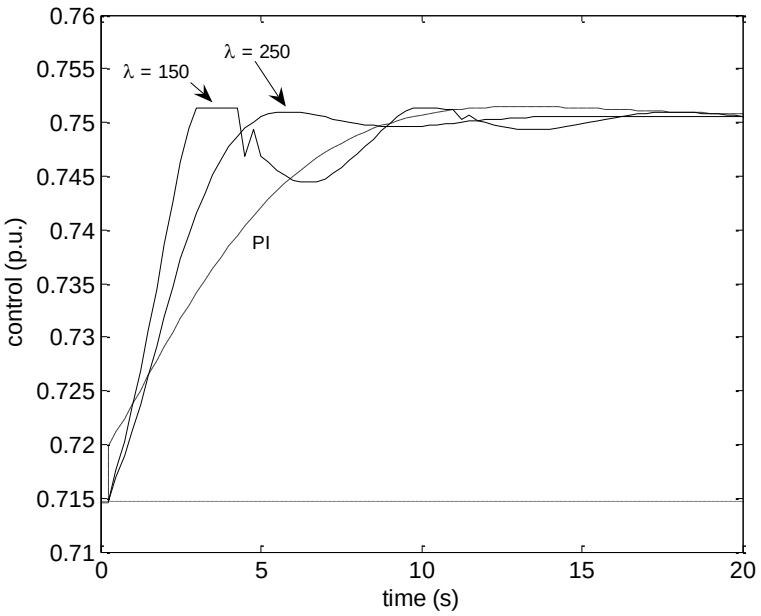

(b)

Figure 6 Comparison of CGPC and PI when all 6 units have a small step demand in power (the results are identical for all 6 units) – (a) responses (b) controls.

The $\lambda = 150$ case now has substantial oscillation and causes the saturation constraint to be activated. CGPC produces an initial control that is slower than PI, which causes a generation delay, but this is followed by a rapid rise in output which is sustained almost to the point where the power reaches the set-point. The response for $\lambda = 250$ has a rather deeper NMP under-shoot than PI control and a slightly under-damped response but it gives several seconds advantage on primary response. For the worst-case of 6 units reacting together (which rarely occurs in practice), $\lambda = 250$ gives a response that is close to the acceptable damping limit. Although the corresponding response for the 1 unit operational case (Figure 4) remains a little conservative, it is a substantial improvement on PI control. A value of $\lambda = 250$ is a suitable compromise for a fixed-parameter controller and is assumed throughout the remainder of the paper.

It is also possible to compare the step response during single unit operation with the specification published by Jones *et al* (2004), which is used for control systems research at

Dinorwig. This specification is more demanding than the station's contractual obligation but is set below the plant's 'hydraulic limit'; it is believed to be near to the plant's optimum dynamic response. Table 1 summarises the 7 tests in the step response specification and the performances achieved by the PI and CGPC controllers (taken from Figure 5).

Table 1 Comparison of PI and CGPC single-unit step responses with the specification

Test	**Criterion**	**Specification**	**PI**	**CGPC (λ = 250)**
P1	Primary response	$P_1 \geq 90\%$ at t_{p1}=10s	81% at 10s, 90% at 13.683s	90% at 8.446s
P2	Overshoot	$P_2 = 5\%$ $t_{p2} \leq 20$s	No overshoot	No overshoot
P3	Settling time	$t_{p3} = 25$s for $P_3 \leq 1\%$	25.927s	14.647s
P4	Time to steady state	$t_{p4} = 60$s for $P_4 \leq 0.5\%$	29.203s	16.294s
P5	Rise time	$t_{p5} = 8$s	12.052s	6.259s
P6	Undershoot	$P_6 \leq 2\%$	1.75%	0.75%
P7	NMP zero crossover time	$t_{p7} \leq 1.5$s	0.88s	1.279s

Table 1 shows that the most significant advantage of CGPC is its primary response, which is 38% faster than the PI case and meets the more demanding specification. It also settles 44% sooner and has an undershoot which is 57% lower. It is concluded that, for small-signal responses simulated on the full plant model, CGPC retains the advantage over PI noted in (Muñoz Hernández and Jones, 2006). It also produces stable and satisfactory responses over the whole operational envelope.

5 Large amplitude ramp responses

Observing small-step responses gives valuable insight into the speed and accuracy of the system in closed loop when it is tracking a power target which, in frequency control mode, is set by the deviation of supply frequency from its nominal 50Hz. However, Dinorwig often operates in 'dead-band' mode, where it is called upon by the grid controller to supply large, rapid power changes (typically 150MW or 0.5p.u. within a few seconds) in order to counteract an upward or downward trend in the supply frequency. This is initiated by a plant operator

and takes the form of a ramp change in the power set-point for one or more Units. A rapid change in generated power is achieved by including a feed-forward path in the governor, as shown in Figure 3. How the CGPC and PI controller compare in this situation is shown in Figure 7 and Figure 8, where P_{ed} is ramped at a rate of 0.0833p.u. (25 MW/s); at this rate the guide vanes move from being closed to fully open in 12s.

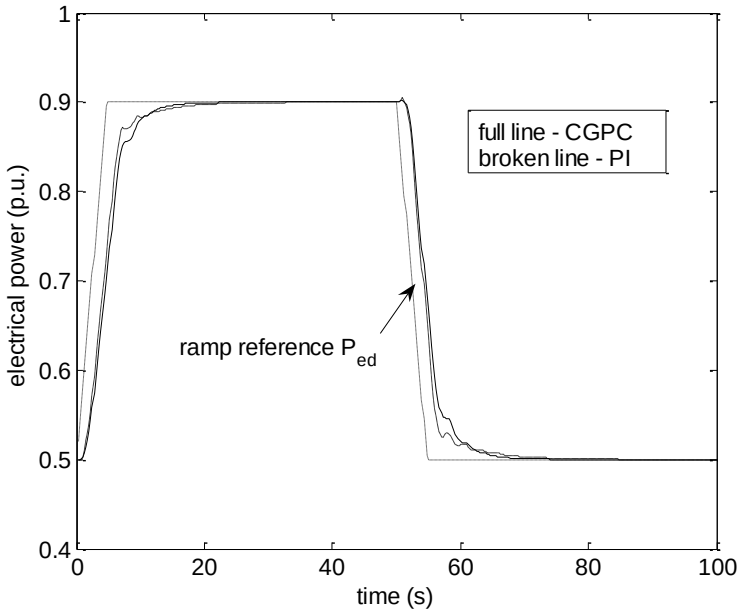

Figure 7 Comparison of CGPC and PI responses with large amplitude ramp on set-point and feed-forward gain; one unit operational.

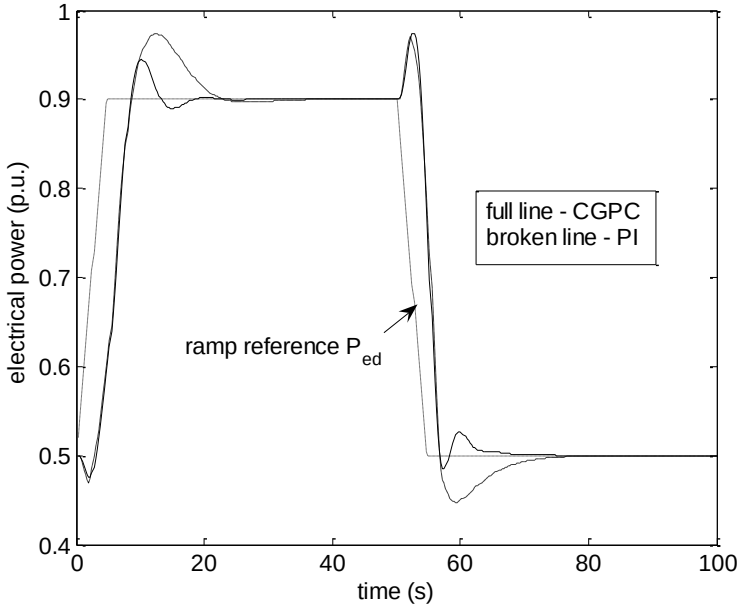

Figure 8 Comparison of CGPC and PI responses with large amplitude ramp on set-point and feed-forward gain; six units operational.

In Figure 7, a single turbine generator is ramped from 0.5p.u. to 0.9p.u. and back, the other units being off-line and the feed-forward gain (K_{ff}) being set at 0.5. CGPC provides a slightly shorter settling time than PI but the differences between the responses are small. When all six units are ramped together, as shown in Figure 8, CGPC yields a smaller overshoot than PI for both positive and negative ramps; the asymmetry in the response is due to the nonlinearity in (1) and (2). This result confirms that CGPC can accommodate large amplitude power changes as well as small changes around a given operating point and that it combines well with feed-forward control in 'dead-band' mode.

6 Sensitivity to change in hydraulic head

As with any pumped storage scheme, the supply head changes over a 24 hour cycle as the level in the upper reservoir rises and falls. At Dinorwig, the hydraulic head generally falls to no lower than 90% of nominal. Figure 9 shows the small-step responses produced by the CGPC and PI controllers for the single unit operational case, where the upper curve in both cases is for 100% head. Again, the CGPC is tuned with $\lambda = 250$ and the PI controller has anti-windup and the standard gain values. As expected, the response with both controllers is slower when the head is reduced but the CGPC responses are closer together than for the PI case, indicating that it is less sensitive to the hydraulic head.

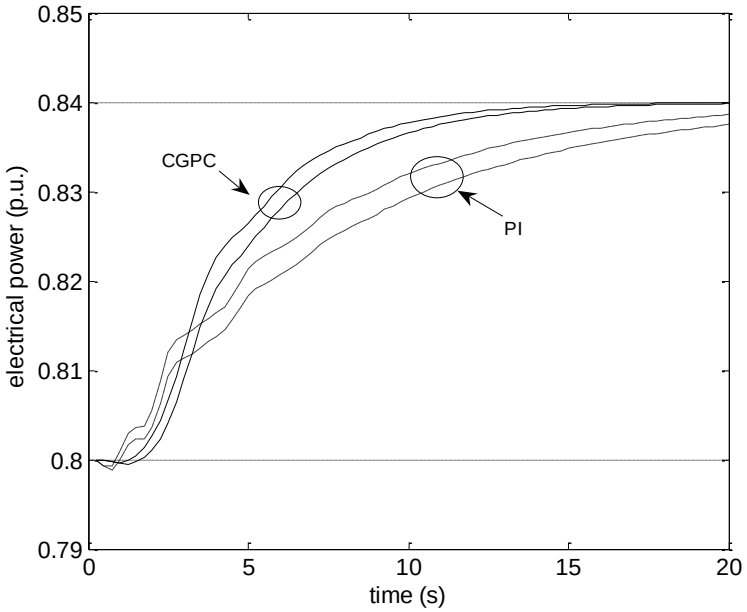

Figure 9 Comparison of CGPC and PI small-step responses with 100% and 90% supply head; single unit operational .

7 Frequency control mode - sensitivity to Grid size.

When one or more units at Dinorwig operates in frequency control mode, it is important that the system be robust to changes in the Grid characteristics, which vary with time of day and with season. In England and Wales, maintenance of the supply frequency is the responsibility of National Grid Transco (NGT), which procures automatic regulation capability from private generators by means of a pricing mechanism known as Ancillary Services. Typically, there will be several regulators, of varying capacity and speed of response, connected to the Grid. Stable sharing of the load between multiple generators is achieved by including a 'droop' characteristic (Kundur, 1994) in their governors. Figure 10 shows that the supply frequency, f_G, is affected by changes in the Grid load, ΔP_L, which are counteracted by the generated electrical power ΔP_e. The role of the hydroelectric station is to provide accurate and timely supply of its target power contribution to the Grid.

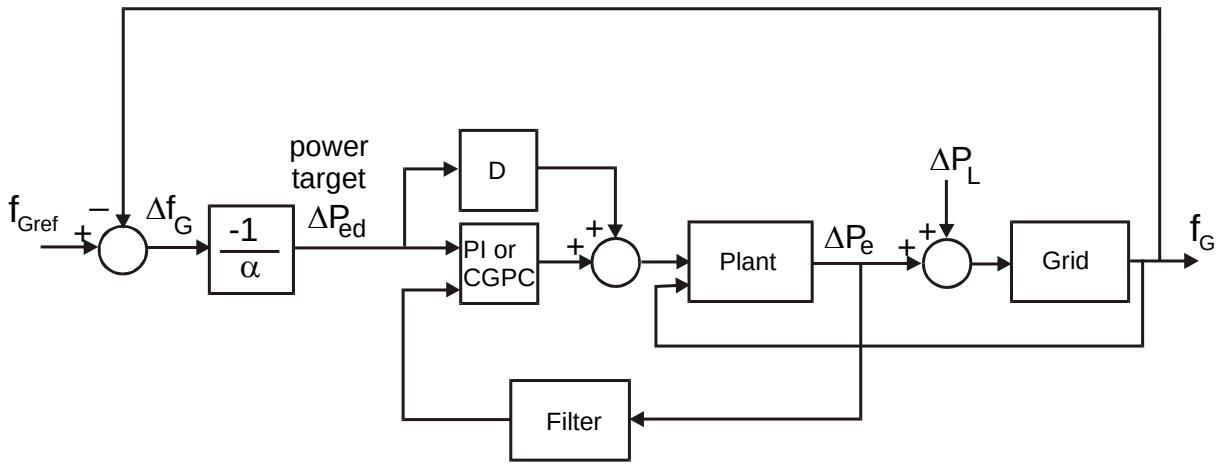

Figure 10 Block diagram for one Unit in automatic frequency control mode (coupling paths to the remainder of the plant are omitted for clarity).

The power target ΔP_{ed} varies in proportion to the Grid frequency error:

$$\Delta P_{ed} = (f_{Gref} - f_G)\frac{P_r}{\alpha f_{Gref}} \tag{10}$$

where P_r is the rated power of the generator (300MW), f_{Gref} is the nominal supply frequency (50Hz) and α is the droop. Then the deviation of Grid frequency from nominal (Δf_G) is:

$$\Delta f_G = (f_G - f_{Gref}) = \frac{-\Delta P_{ed}\alpha\, f_{Gref}}{\Delta f_G} \tag{11}$$

and:

$$\frac{\Delta P_{ed}}{P_r} = -\frac{1}{\alpha}\frac{\Delta f_G}{f_{Gref}} \quad or \quad \Delta P_{ed}(p.u.) = -\frac{1}{\alpha}\Delta f_G(p.u.) \tag{12}$$

In Figure 10, the block representing Grid dynamics is based on the derivation by Anderson & Mirheydar (1990). Their model assumes that the Grid response is dominated by two time constants, one associated with the sum of all the inertias of the rotating machines and the other associated with all regulatory mechanisms connected to the grid, assumed to be primarily re-heat steam turbine generators. This gives a second order transfer function relating Grid frequency to total active power imbalance:

$$\Delta f_G = \frac{\omega_n^2 T_R}{\beta}\left(\frac{s + 1/T_R}{s^2 + 2\zeta\omega_n s + \omega_n^2}\right)(\Delta P_e - \Delta P_L) \tag{13}$$

In (13), ω_n and ζ are the natural frequency and damping factor of the Grid, T_R is the aggregate time constant of steam reheat plant and β is the power system stiffness (i.e. the inverse of the steady-state sensitivity of frequency to changes in input power). Values for these parameters have been identified as an ARMAX (auto-regressive moving-average and exogenous variable) model from data measured at Dinorwig (Jones, 2004), (Jones, 2005).

Figure 11 shows both CGPC and PI responses when a step load increase (ΔP_L) is applied to the Grid, for a condition when five Units are generating at full-load in dead-band mode and the remaining Unit is in frequency-control mode. The Grid parameters are taken as ± twice the standard deviation from the mean values obtained in (Jones, 2005), so that the upper graph corresponds to a very 'weak' Grid (ω_n = 0.17r/s, ζ = 0.27 and β = 3.62p.u.) and the lower graph to a very 'stiff' Grid (ω_n = 0.48r/s, ζ = 0.91 and β = 15.5p.u.). Note that both the steady-state and dynamic characteristics of the electrical power output are affected.

In Figure 11, the power target (ΔP_{ed}) is similar for the CGPC and PI cases because it is a function of the aggregate Grid regulation and only partially influenced by the Dinorwig contribution, ΔP_e. For both extremes of Grid characteristics, CGPC gives better tracking of the demanded power than PI and, in the case of the 'stiff' Grid, it is also a smoother response. Although CPGC delivers more of the demanded power than PI control, the inherent delay associated with the NMP characteristic of the hydraulics is very evident. This cannot be reduced further by feedback and alternative methods such as the use of predictive feed-forward (the block K_{ff} in Figure 3) have been suggested to counteract this effect (Jones and Mansoor, 2004).

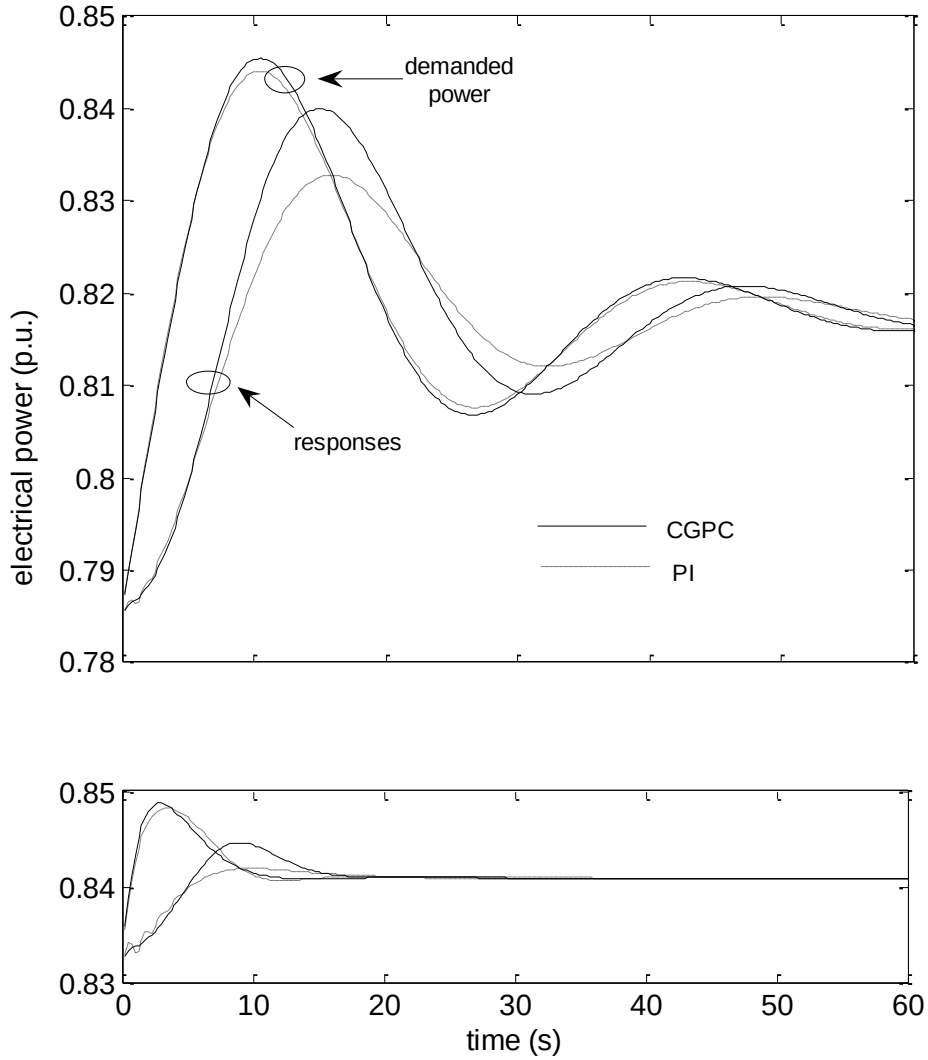

Figure 11 Responses to a 0.0015p.u. step load increase on the Grid for two sets of parameters – upper figure for a 'weak' Grid and lower figure for a 'stiff' Grid.

It may be concluded that CGPC retains its advantage over the range of Grid conditions likely to be encountered in practice and that this is not obtained simply by being better 'tuned' than the PI controller to a nominal set of Grid parameters.

8 CGPC real-time computation

As noted at the end of Section 3, the computation time for CGPC is substantially greater than GPC because of the nonlinear search algorithm employed. Moreover, the computation is

unbounded, which is not acceptable for a real-time system. Clearly, the sustainable sample rate depends both on the complexity of the algorithm and the hardware implementation. A comparative measure of the computation times of CGPC and GPC executing on the same platform may be obtained by recording the start and stop times of the control calculation, using the in-built Matlab timer functions. A simulation was set up where the power reference was varied in small and large steps and ramps, sufficient to activate the CGPC control constraints over some segments of the simulation interval. Figure 12 shows how the control loop time varied over the simulation interval for GPC, CGPC and the case of CGPC limited to 5 iterations of the QP search.

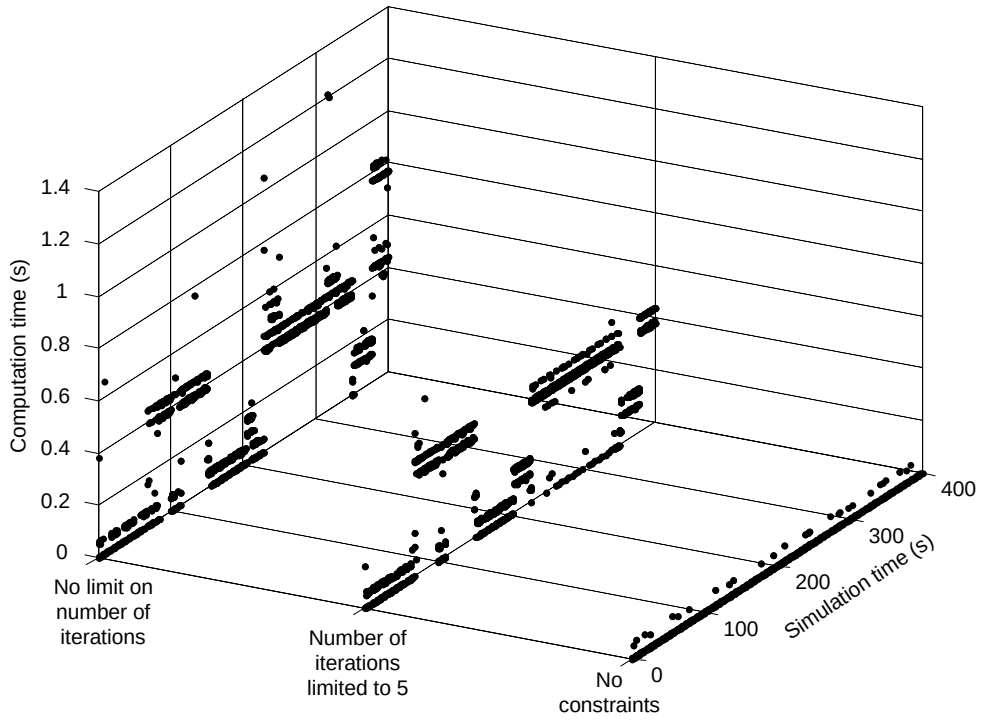

Figure 12 Comparison of computation times for the GPC algorithm, showing the effect of QP search iterations needed in the constrained version.

As expected, the loop time for the GPC controller is small and constant whereas the loop times for CGPC are much longer. In the case of unlimited iterations, the loop times are variable but when the number of iterations is limited to 5, the loop time remains much greater than GPC but is bounded. This is summarised in Table 2.

Table 2 Comparison of computation times for the GPC algorithm

Algorithm	Average (s)	Maximum (s)
GPC	0.001	0.02
CGPC limited to 5 iterations	0.115	0.36
CGPC unlimited iterations	0.214	1.56

The plant responses for the two CGPC cases were compared over the simulation period and were found to be virtually identical, with a significant discrepancy only occurring in the extreme case of the six units being ramped from zero to full load together. It is concluded that only a small number of QP iterations need be done to realise almost all the benefit of the CGPC algorithm. The maximum loop time of 360ms in Table 2 is an order of magnitude greater than the 40ms sample rate used on the Dinorwig governors. However, this is a measurement made in Simulink's off-line interpretive simulation mode and is subject to considerable overhead. Speed gains of the order of 5-20 times can be achieved by re-writing S-functions in the C language. A further 2-10 times speed gain can be achieved if Real-Time Workshop (MathWorks, 2006) is used to generate optimised and model-specific code, which can then be compiled. If necessary, dedicated hardware such as DSPs or FPGAs could give an order-of-magnitude reduction of the computing time, although this would lead to increased development costs and require interfacing to the industrial PLC used to implement the governor.

9 Conclusions

The results presented here have confirmed, using the most comprehensive simulation of Dinorwig currently available, that CGPC has the potential to improve performance across the operating envelope. Taking explicit account of the multivariable nature of the plant improves both the direct and cross-coupled transient responses, compared with PI control. Inclusion of rate and saturation constraints in CGPC yields a fast, well-damped response in the commonly-occurring case of single Unit operation, without compromising stability when multiple Units

are on-line. CGPC retains its advantage in the case of large ramp responses and changing hydraulic head and improves power target tracking in frequency-control mode. It is worth emphasising that the PI controller used for comparison includes saturation and anti-windup features. The close relationship which is known to exist between anti-windup PI and MBPC (De Dona, Goodwin et al., 2000) makes it a much more realistic competitor to CGPC than a basic PI realisation. Nevertheless, CGPC remains a fixed-parameter controller so current work is investigating how it can be extended as a mixed logical/dynamic (MLD) controller (Muñoz Hernández, Jones et al., 2005) whose components, such as the predictive model and 'inverse gain' λ, vary according to operating condition. MLD also has the potential to include higher level plant functions (such as financial or maintenance data) in the cost function and offers an integrated control system solution applicable across a range of operational scenarios.

Although this work is a significant step towards practical implementation of CGPC on the plant, it is unlikely that this will occur until the next major revision of governor hardware. The financial penalty which accompanies any loss of operational capability is the greatest factor that limits experimental development but practical and technical restrictions, such as the need to install synchronized communication (e.g. CAN bus) between the individual Unit governors, is also a constraint. In the meantime, this work has provided Dinorwig (and similar hydroelectric stations) with an early assessment of the potential of CGPC and valuable tuning guidelines for implementation.

Acknowledgements

The authors wish to thank F.C. Aris (Consultant), G.R. Jones (First Hydro Company) and S.P. Mansoor (University of Wales, Bangor) for their assistance. G.A. Muñoz-Hernández wishes to thank *Programa ANUIES-SUPERA* and the *Instituto Tecnológico de Puebla* who supported him in his postgraduate studies.

References

Anderson, P. M. and M. Mirheydar 1990: A low-order system frequency response model. IEEE Trans Power Systems 5(3), 720-729.

Camacho, E. F. and C. Bordons 1999: Model Predictive Control, Springer-Verlag.

Clarke, D. W., C. Mohtadi, et al. 1987: Generalized predictive control - I The basic algorithm. Automatica 23 137-148.

Clarke, D. W., C. Mohtadi, et al. 1987: Generalized predictive control - II Extensions and interpretations. Automatica 23 149-160.

De Dona, J. A., G. C. Goodwin, et al. 2000: Anti-windup and model predictive control : Reflections and connections. European Journal of Control 6 467-477.

IEEE Working group 1992: Hydraulic turbine and turbine control models for system dynamic studies. IEEE Trans Power Systems 7(1), 167-179.

Jones, D. I. 1999: Multivariable control analysis of a hydraulic turbine. Trans Inst MC 21(2/3), 122-136.

Jones, D. I. 2004: Estimation of power system parameters. IEEE Trans Power Systems 19(4), 1980-1989.

Jones, D. I. 2005: Dynamic parameters for the National Grid. Proc IEE Gener. Transm. Distrib. 152(1), 53-60.

Jones, D. I. and S. P. Mansoor 2004: Predictive feed-forward control for a hydroelectric plant. IEEE Trans Control Systems Technology 12(6), 956-965.

Jones, D. I., S. P. Mansoor, et al. 2004: A standard method for specifying the response of hydroelectric plant in frequency-control mode. Electric Power Systems Research 68(1), 19-32.

Kundur, P. 1994: Power System Stability and Control, McGraw Hill.

Maciejowski, J. M. 2001: Predictive Control with constraints, Prentice Hall.

Mansoor, S. P., D. I. Jones, et al. 2000: Reproducing oscillatory behaviour of a hydroelectric power station by computer simulation. Control Engineering Practice 8 1261-1272.

MathWorks 2006: Real-Time Workshop. Natick, USA.

Muñoz Hernández, G. A. and D. I. Jones 2004. Applying generalised predictive control to a pumped-storage hydroelectric power station. Proc 23rd IASTED Int Conf Modelling, Identification & Control. Grindelwald, Switzerland**:** 380-385.

Muñoz Hernández, G. A. and D. I. Jones 2004. Modelling, simulation and control of a pumped storage hydroelectric power station. Proc UKACC Conf CONTROL'04. Bath, UK**:** ID-214.

Muñoz Hernández, G. A. and D. I. Jones 2006: MIMO generalised predictive control for a hydroelectric power station. IEEE Trans Energy Conversion 21(4), 921-929.

Muñoz Hernández, G. A., D. I. Jones, et al. 2005. Evaluation of MLD predictive control in a nonlinear model of a power station. Proc 16th IASTED Conference on Modelling & Simulation. Cancun, Mexico**:** paper 459-076.

Richalet, J. 1993: Industrial applications of model based predictive control. Automatica 29 1251-1274.